A Distributed Control Strategy Based on DC Bus Signaling for Modular Photovoltaic Generation Systems With Battery Energy Storage

Kai Sun, Li Zhang, Yan Xing, *Member, IEEE*, and Josep M. Guerrero, *Senior Member, IEEE*

***Abstract*—Modular generation system, which consists of modular power conditioning converters, is an effective solution to integrate renewable energy sources with conventional utility grid to improve reliability and efficiency, especially for photovoltaic generation. A distributed control strategy based on improved dc bus signaling is proposed for a modular photovoltaic (PV) generation system with battery energy storage elements. In this paper, the modular PV generation system is composed of three modular dc/dc converters for PV arrays, two grid-connected dc/ac converters, and one dc/dc converter for battery charging/discharging and local loads, which is available of either grid-connected operation or islanding operation. By using the proposed control strategy, the operations of a modular PV generation system are categorized into four modes: islanding with battery discharging, grid-connected rectification, grid-connected inversion, and islanding with constant voltage (CV) generation. The power balance of the system under extreme conditions such as the islanding operation with a full-charged battery is taken into account in this control strategy. The dc bus voltage level is employed as an information carrier to distinguish different modes and determine mode switching. Control methods of modular dc/dc converters, battery converter, and grid-connected converter are addressed. An autonomous control method for modular dc/dc converters is proposed to realize smooth switching between CV operation and maximum power point tracking operation, which enables the dc bus voltage regulation capability of modular dc/dc converters. Seamless switching of a battery converter between charging and discharging and that of a grid-connected converter between rectification and inversion are ensured by the proposed control methods. Experiments verify the practical feasibility and the effectiveness of the proposed control strategies.**

***Index Terms*—Battery energy storage, dc bus signaling (DBS), distributed control, modular system, photovoltaic (PV) generation.**

Manuscript received November 5, 2010; revised January 21, 2011; accepted January 27, 2011. Date of current version October 12, 2011. This work was supported in part by the Power Electronics Science and Education Development Program of Delta Environmental and Educational Foundation under Grant DREG2010007, in part by the State Key Laboratory of Power Systems, Tsinghua University, China, under Grant SKLD09M15, and in part by the Transformation of Scientific and Technological Achievements in Jiangsu, China, under Grant BA2008001. Recommended for publication by Associate Editor K. Ngo.

K. Sun is with State Key Laboratory of Power Systems, Department of Electrical Engineering, Tsinghua University, Beijing 100084, China (e-mail: sunkai@mail.tsinghua.edu.cn).

L. Zhang and Y. Xing are with Jiangsu Key Laboratory of New Energy Generation and Power Conversion, College of Automation Engineering, Nanjing University of Aeronautics and Astronatutics, Nanjing 210016, China (e-mail: zhanglinuaa@nuaa.edu.cn; xingyan@nuaa.edu.cn).

J. M. Guerrero is with the Department of Automatic Control Systems and Computer Engineering, Universitat Politecnica de Catalunya, 08036 Barcelona, Spain and also with the Department of Energy Technology, Aalborg University, Aalborg 9220, Denmark (e-mail: josep.m.guerrero@upc.edu, joz@et.aau.dk).

Color versions of one or more of the figures in this paper are available online at http://ieeexplore.ieee.org.

Digital Object Identifier 10.1109/TPEL.2011.2127488

I. Introduction

DURING recent years, the utilization of renewable energy sources has been promoted quickly to fulfill increasing energy demand and deal with global climate change. Since the distributed power generation by renewable energy has different characteristics with conventional power generation by fossil fuels, novel configurations, topologies, and control techniques are employed to integrate renewable energy sources with utility grid [1]–[6]. As the cost decreases continuously, photovoltaic (PV) generation has become one of the most important renewable energy sources and has been widely used. A review of grid-connected inverters for PV modules shows that there are four topologies used in PV generation systems as shown in Fig. 1 [6]. Considering cost and efficiency, multistring topology is one of the most widely used solutions for PV generation as well as ac module topology [6], [7]. As shown in Fig. 1(c), the dc–dc converters for each string of PV modules can be implemented with a modular design and share a dc bus, which connects an ac utility grid through a dc–ac converter. This configuration has the potential to be extended to a dc bus-based modular PV generation system; not only the modular dc/dc converters and dc/ac converters, but also the energy storage devices and local loads can be connected through a dc bus. It will be an effective solution for the future applications of PV generation.

Due to the stochastic characteristic of PV generation, energy storage elements are indispensable to smooth the power flow and provide the electric energy with high quality. Lots of efforts have been carried out by the researchers on the integration and coordination of PV generation and energy storage elements. Multifunctional power converters are developed to integrate batteries as the backup for PV generation systems [8], [9]. PV generation and battery are used coordinately to feed utility grid or plug-in hybrid electric vehicle load [10]–[12]. In these works, different power conditions and battery capacity limit are taken into account, but the islanding operation has not been considered. In grid-connected PV systems, the incorporation of battery storage can improve the energy production, especially in the presence of mismatching conditions. However, the upper/lower limits of state of charge (SoC) for batteries are usually ignored [13], [14], which influences the effective utilization of battery storage. In order to minimize the demanded battery capacity, the so-called smoothing effect has been investigated, which dumps the power flow fluctuation by using multi-PV systems with different

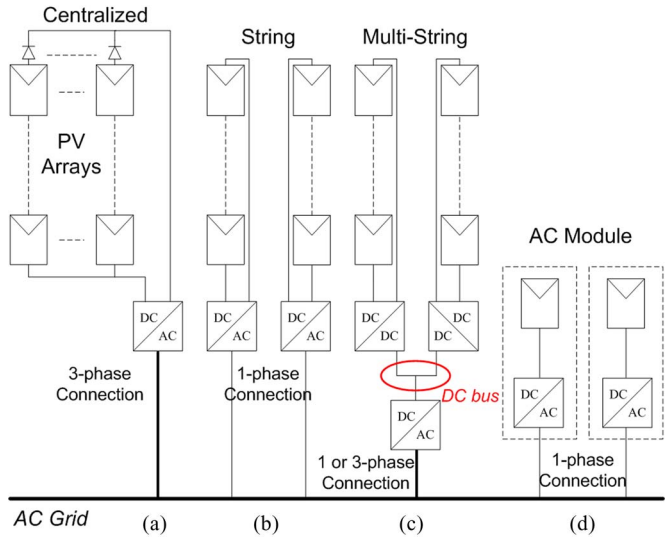

Fig. 1. Configurations of PV generation systems.

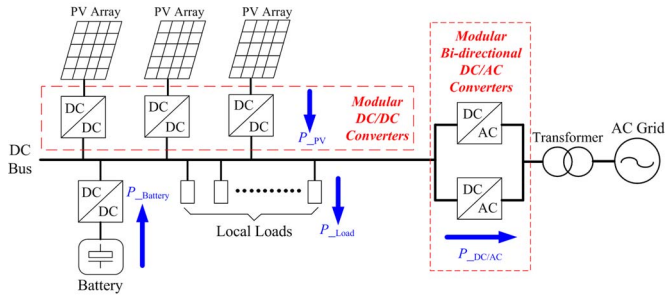

Fig. 2. DC bus-based modular PV generation system.

locations [15]. Besides batteries, fuel cells are also employed to smooth the energy production profile of grid-connected PV systems [16], [17]. Although the control flexibility can be improved by diverse energy storage elements, high cost is still a critical issue for the generation system. Some stand-alone PV generation systems with energy storage are developed for residential and rural applications [18]–[21]. In these systems, the SoC limits of batteries during islanding operation are considered, but grid-connected power flow is not taken into account. The hybrid energy storage system, which consists of batteries and supercapacitors, is used to optimize the energy utilization and minimize the energy storage capacities [18], [19]. Only a few literatures mention the control of a dc bus-based modular PV system with a battery [22], but the detailed power management scheme and the SoC limits are not presented.

Based on the aforementioned review of previous works, it can be found that the pieces of research on power management control for a modular PV generation system are very rare and the existing control techniques cannot be moved to a modular PV generation system directly. In order to fulfill the requirements by distributed generation and optimize the energy utilization, the control of modular PV generation systems with battery storage must have the following functions: 1) the reasonable power distribution among different modular converters should be ensured, 2) the system can be operating either at grid-connected mode or at islanding mode; and 3) the SoC limits (full-charged or full-discharged) of batteries must be considered.

To enhance the system reliability, a distributed control strategy so-called dc bus signaling (DBS) was applied for a hybrid renewable nanogrid [23], [24]. DBS is an extension of the concept of using charge/discharge thresholds to schedule individual sources in a distributed fashion, which induces dc bus voltage level changes to realize the communications between difference source/storage interface converters. By using DBS, the system reliability can be inherently maintained since the dc bus itself is used as the communication link [24]. However, this control strategy cannot be applied for a modular PV generation system directly, because: 1) the interaction with ac utility grid is not included; 2) the control method is developed for individual renewable sources, but not for modular sources; and 3) some extreme conditions such as the islanding operation with a full-charged battery are not mentioned, which means that the power regulation capability of a battery is deteriorated.

In this paper, the DBS method has been improved for both grid-connected operation and islanding operation. A novel distributed control strategy based on DBS is proposed for the modular PV generation system. The configuration of a dc bus-based modular PV generation system with ac grid connection and battery storage is presented in Section II. A power management scheme taking full-charged battery conditions into account and control methods for modular dc/dc converters, grid-connected converters, and battery converter are addressed in Section III. Experimental results are shown in Section IV and Section V concludes the works.

II. System Configuration

The dc bus-based modular PV generation system investigated in this paper is shown in Fig. 2. Three modular dc/dc converters for PV arrays, two modular bidirectional dc/ac converters, a bidirectional dc/dc converter for a battery, and local loads share a dc bus. The modular dc/dc converters are the key elements in this system, which are implemented with modular design and same ratings. These modular dc/dc converters transfer the power generated by PV arrays to a dc bus. The modular bidirectional dc/ac converters are used to connect the dc bus and ac utility grid, which enable bidirectional power flow. The battery with a bidirectional dc/ac converter is used to balance the power differences between PV power supplies and local loads in islanding mode. The local loads include the auxiliary power supplies for system operations, such as control/monitoring of PV arrays, battery monitoring, and control/driving of converters.

Since the elements and devices in this system can be summarized into three categories, energy generation unit, energy storage unit, and loads, the configuration shown in Fig. 2 can be considered as a typical case of dc microgrid with renewable generation and energy storage. The control strategies developed for this system can also be applied to dc microgrids.

III. Distributed Control Strategy

The distributed control strategy for a modular PV generation system consists of a power management scheme with DBS and the control methods for power converters.

A. Power Management Scheme With DC Bus Voltage Signaling

In this paper, a power management scheme with dc bus voltage signaling is proposed to maintain the power balance and stable operation of the system under any conditions. In this scheme, the operation of the modular PV generation system is categorized into four modes: Mode I (islanding mode with battery discharging), Mode II (grid-connected mode with rectification), Mode III (grid-connected mode with inversion), and Mode IV (islanding mode with dc bus voltage regulation by PV). These four operation modes are identified by different dc bus voltage levels, which means that the dc bus voltage is used as an information carrier. The switching between different modes and the corresponding changes of control methods for converters can be achieved through dc bus voltage changes without additional communication links. This benefits cost reduction and reliability enhancement.

Four operation modes are described as follows.

The nominal dc bus voltage in this system is $V_{\mathrm{dc}\_n} = 200\,\mathrm{V}$ and different reference dc bus voltages $V_{\mathrm{dc\_ref}}$ indicate different operation modes.

1) *Mode I:* $V_{\mathrm{dc\_ref}} = 0.9V_{\mathrm{dc}\_n} = 180\,\mathrm{V}$. In this mode, the system operates in islanding mode and the dc bus voltage is regulated by battery discharging, which means that the generated PV power is less than local load demands. The modular dc/dc converters for PV arrays work with maximum power point tracking (MPPT) and the grid-connected bidirectional dc/ac converters are disabled. Hence, this mode is called as the islanding mode with battery discharging.
2) *Mode II:* $V_{\mathrm{dc\_ref}} = 0.95V_{\mathrm{dc}\_n} = 190\,\mathrm{V}$. In this mode, the system operates with connection to ac grid through bidirectional dc/ac converters. The dc bus voltage is regulated by the dc/ac converters through rectification, which means that the generated PV power is less than local load demands. The modular dc/dc converters for PV arrays work with MPPT. If the battery has been fully charged, the dc/dc converter for the battery does not work; otherwise the dc/dc converter is used to charge the battery. Hence, this mode is called as the grid-connected mode with rectification.
3) *Mode III:* $V_{\mathrm{dc\_ref}} = V_{\mathrm{dc}\_n} = 200\,\mathrm{V}$. In this mode, the system operates with connection to ac grid through bidirectional dc/ac converters. The dc bus voltage is regulated by the dc/ac converters through inversion, which means that the generated PV power is greater than the local load demands. The modular dc/dc converters for PV arrays work with MPPT. If the battery has been fully charged, the dc/dc converter for the battery does not work; otherwise the dc/dc converter is used to charge the battery.
4) *Mode IV:* $V_{\mathrm{dc\_ref}} = 1.05V_{\mathrm{dc}\_n} = 210\,\mathrm{V}$. In this mode, the system operates in islanding mode and the dc bus voltage is regulated by modular dc/dc converters for PV arrays. Since the maximum power of PV arrays in this mode is greater than the local load demands, the modular dc/dc converters for PV modules must not be all operating with MPPT. Actually, one of these modular converters is operating with constant voltage (CV) control. If the battery has been fully charged, the dc/dc converter for the battery does not work; otherwise the dc/dc converter is used to charge the battery. The grid-connected bidirectional dc/ac converters do not work. Hence, this mode is called as the islanding mode with dc bus voltage regulation by PV.

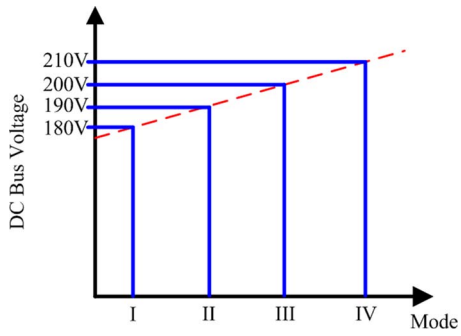

Fig. 3. Operation modes with corresponding dc bus voltage levels.

The operation modes with corresponding dc bus voltage levels are illustrated in Fig. 3. The coefficient difference between different mode voltages is set at 0.05 (0.9, 0.95, 1.0, and 1.05). This is determined based on the following considerations: 1) the voltage difference between different modes must not be too small; otherwise, the malfunction of mode switching will occur due to the sampling inaccuracies and external disturbance; 2) the voltage difference between different modes should not be too large; otherwise, the converters will operate with low voltage and high current, which will probably result in low efficiency and overcurrent faults. Hence, the voltage difference is set at 10 V, which means that the coefficient difference is 0.05 (=10 V/200 V).

The functions of dc/dc converters and dc/ac converters in different modes are summarized in Table I. The converter regulating dc bus voltage, which works as a voltage source, is defined as the dc bus forming unit; the converter providing power with dc bus, which works as a current source, is defined as the dc bus feeding unit; the converter absorbing power from the dc bus is defined as the load unit.

The power flows of the dc/ac converters and battery converter are listed in Table II, where the positive directions of power flows are defined in Fig. 2.

Generally, the system works at Mode III to utilize PV power fully during the daytime. When the sunshine is insufficient like nighttime or cloudy days, the system moves to Mode II to maintain power balance by using the power from ac grid. Only while the faults occur at ac utility grid, the system has to be disconnected with it. During the islanding operation, the system works at Mode I or Mode IV depending on the PV power conditions (lower or higher than load demands). Thus, the battery energy is only used to feed loads at emergent cases without grid

TABLE I
FUNCTIONS OF POWER CONVERTERS UNDER DIFFERENT OPERATION MODES

	Mode I	Mode II	Mode III	Mode IV
DC bus forming	Battery converter (discharging)	Grid-connected converter (rectification)	Grid-connected converter (inversion)	PV converter (constant voltage generation)
DC bus feeding	PV converter (MPPT generation)	PV converter (MPPT generation)	PV converter (MPPT generation)	PV converter (MPPT generation)
DC bus Loading	-	Battery converter (charging)	Battery converter (charging)	Battery converter (charging)

TABLE II
POWER FLOW UNDER DIFFERENT OPERATION MODES

Mode	Islanding/ Grid-connection	Power flow of DC/AC converters	Power flow of battery converters
I	Islanding	$P_{\_DC/AC}$=0	$P_{\_Battery}$>0
II	Grid-connection	$P_{\_DC/AC}$<0	$P_{\_Battery}$<0 or =0
III	Grid-connection	$P_{\_DC/AC}$>0	$P_{\_Battery}$<0 or =0
IV	Islanding	$P_{\_DC/AC}$=0	$P_{\_Battery}$<0 or =0

connection and the battery capacity should be designed to support the islanding operation with enough time required by users.

B. Equivalent Circuits and Analysis

In order to analyze the system operation clearly, the equivalent circuits have been depicted in Fig. 4 by using the Thevenin theorem and Norton theorem.

In Mode I, all the PV converters with MPPT can be considered as current sources and the battery converter works as a voltage source to regulate the dc bus voltage.

Fig. 4(b) shows a typical case of Mode II. In Mode II, all the PV converters work with MPPT, which are considered as current sources. Only one dc/ac converter works with nonfull power rectification to regulate the dc bus voltage, which is considered as a voltage source. The other dc/ac converter works with full power rectification, which is considered as a current source, or at standby mode according to the power conditions. The battery is charged with constant current until it has been fully charged. The control methods for dc/ac converters and battery converter are presented in Section III-C in detail.

The condition in Mode III is similar to Mode II, as shown in Fig. 4(c). In Mode III, all the PV converters work with MPPT, which are considered as current sources. Only one dc/ac converter works with nonfull power inversion to regulate the dc bus voltage, which is considered as a voltage source. The other dc/ac converter works with full power inversion, which is considered as a current source, or at standby mode according to the power conditions. The battery is charged with constant current until it has been fully charged. The control methods for dc/ac converters and a battery converter are presented in Section III.-C in detail.

Fig. 4(d) shows a typical case of Mode IV. Only the PV converter with CV control works as a voltage source, and other PV converters with MPPT work as current sources. The battery is charged with constant current until it has been fully charged.

According to the aforementioned analysis, it can be found that at any time only one voltage source operates in each mode and all of the other converters work as current sources, which means that the dc bus voltage can be regulated at constant in each mode. This characteristic ensures the system stability.

C. Control Methods for DC/DC Converters and DC/AC Converters

1) Combined Control Method for Modular PV DC/DC Converters: Each modular dc/dc converter for PV arrays has two control modes: MPPT control and CV control. The control diagram is shown in Fig. 5. $V_{\rm dc}$ is the actual dc bus voltage and $V_{{\rm dc}\_d}$ is the detected dc bus voltage. K_d is the sampling coefficient for dc bus voltage detection, which depends on the parameter of sampling circuits. Even though the dc/dc converters for PV arrays are implemented with modular design, they still have some small differences in the values of K_d due to the component parameter errors in sampling circuits. $V_{\rm dc\_ref} = 210$ V is the reference voltage for a dc bus in Mode IV. $V_{\rm pv}$ and

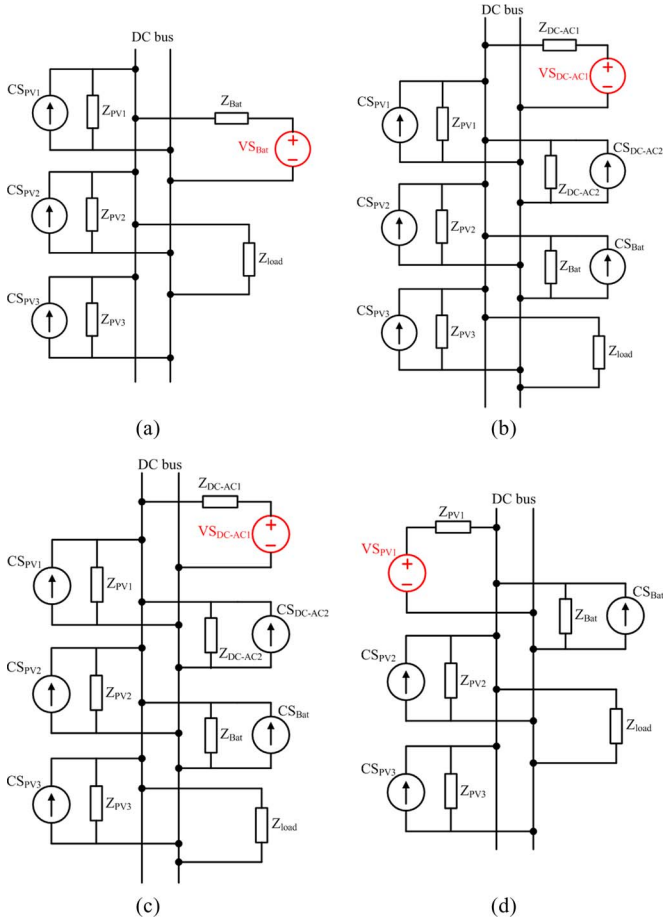

Fig. 4. Equivalent circuits of the system under different modes: (a) Mode I, (b) Mode II, (c) Mode III, and (d) Mode IV.

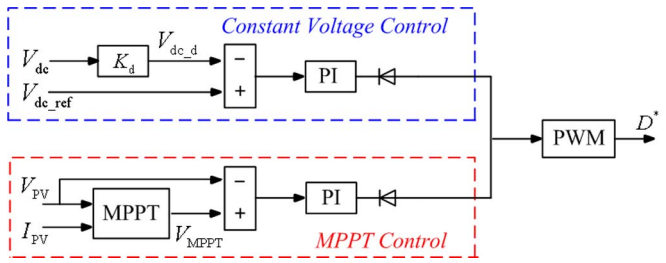

Fig. 5. Control diagram of each modular dc/dc converter for a PV array.

$I_{\rm pv}$ are the output voltage and output current of PV modules, respectively. $V_{\rm MPPT}$ is the reference voltage for the PV array. D^* is the reference duty ratio for dc/dc converters.

When the system is operating in Modes I, II or III, the modular dc/dc converters are controlled with MPPT as current sources. In these modes since the dc bus voltage are regulated within 180–200 V, the output of CV control reaches its positive saturation and has been disabled. When the system works in islanding mode and the generated PV power is greater than the local load, the extra power will be used to charge a battery. If the battery has been fully charged, which means that SoC reaches 95%, the dc bus voltage will increase. If the dc bus voltage reaches 210 V, the CV controller of the modular dc/dc converter with maximum K_d

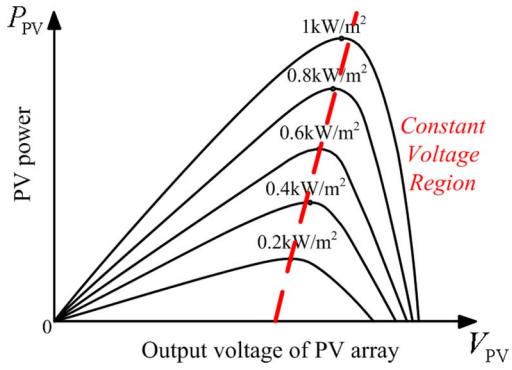

Fig. 6. *P–V* curve of a PV array.

will escape from positive saturation first and begin to regulate the dc bus voltage as $V_{\rm dc\_ref} = 210$ V, while the MPPT controller has been disabled. The modular dc/dc converter with maximum K_d reduces its output power and controls the output voltage of the PV array at a constant value. Thus, the system moves to Mode IV. As shown in Fig. 6, when the modular dc/dc converter is operated with CV control, the corresponding PV array must work within the right region divided by the dash line.

If the dc bus voltage increases continuously, the CV controller of the modular dc/dc converter with maximum K_d will reach negative saturation (zero) and not provide energy with a dc bus. Until a modular dc/dc converter for the PV array with a CV control makes the power balance for the system, the dc bus voltage will be kept at 210 V. At this time, the sampling coefficient of this modular dc/dc converter is defined as $K_{\rm dm}$. The CV controller outputs of the modular dc/dc converters with the sampling coefficients higher than $K_{\rm dm}$ are zero and these converters do not supply energy with a dc bus. The CV controller outputs of the modular dc/dc converters with the sampling coefficients lower than $K_{\rm dm}$ are at positive saturation because $V_{\rm dc\_ref} > K_d * V_{\rm dc}$ and these converters work with MPPT control.

Hence, it is possible to realize that only one modular dc/dc converter works as a voltage source and other converters work in standby mode or as current sources based on the aforementioned control method. The key point is the inherent differences of sampling coefficients. In this control method, the basis for mode switching between CV control and MPPT is that the CV controller reaches its positive saturation or not.

If the dc bus voltage decreases resulting from PV power reduction or local load increases, another modular dc/dc converter will change the operation mode from standby to CV control for power balance. If all the modular dc/dc converters have been working with MPPT and the dc bus voltage decreases to 180 V, the battery dc/dc converter will start and provide energy with a dc bus by discharging. Then, the system moves to Mode I.

2) Control Methods for Grid-Connected DC/AC Converters: When ac utility grid is normally operating, the modular PV generation system will be connected to ac grid through the bidirectional dc/ac converters; otherwise, it will be disconnected with ac grid to avoid faults occurring. The control for grid-connected dc/ac converters includes two levels: 1) parallel control method

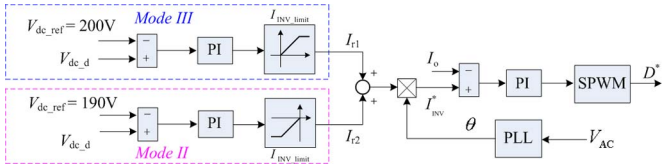

Fig. 7. Local control diagram of a grid-connected dc/ac converter.

for modular grid-connected dc/ac converters; and 2) local control method for one grid-connected dc/ac converter.

The parallel control method proposed in [25] has been employed in this paper. By using this method, only one modular grid-connected dc/ac converter works with nonfull load at a moment, while others work with full load or at standby mode. As power increases, the modular dc/ac converters enter full load operation gradually depending on the dc bus sampling coefficients.

The local control method is shown in Fig. 7. In Fig. 7, $V_{\mathrm{dc\_ref}}$ is the reference voltage for a dc bus, $V_{\mathrm{dc\_}d}$ is the detected dc bus voltage, $I_{\mathrm{INV\_limit}}$ is the maximum current limit for a dc/ac converter corresponding to its power rating, V_{ac} is the ac grid voltage, θ is the ac grid phase angle, I^*_{INV} is the reference output current for a dc/ac converter, I_o is the detected output current of a dc/ac converter, and D^* is the duty ratio for a dc/ac converter. When the system works in Mode II, the local load demands need to be supplied by the PV-generated power and the power from the ac grid through the dc/ac converters. In Mode II, the dc bus voltage is regulated at 190 V by the rectification operation of the dc/ac converters. When the system works in Mode III, the PV-generated power is greater than the local load and extra power will be transferred to the ac grid through the dc/ac converters. In Mode III, the dc bus voltage is regulated at 200 V by the inversion operation of the dc/ac converters. As shown in Fig. 6, the seamless switching between Mode II and Mode III can be realized

$$I^*_{\mathrm{INV}} = (I_{r1} + I_{r2}) * \sin(\theta). \tag{1}$$

3) Control Method for a Battery DC/DC Converter: In Mode I, the battery dc/dc converter is employed as the dc bus forming unit to regulate the dc bus voltage by battery discharging. If the battery has not been fully charged, which means that its SoC is less than 95%, the battery will be charged in Mode II, Mode III, and Mode IV. Considering the aforementioned conditions, the control method for a battery dc/dc converter is summarized in Fig. 8. In Fig. 8, V_B is the detected battery voltage, V_{BH} is the battery voltage corresponding to 95% SoC, V_{BL} is the battery voltage corresponding to 40% SoC, $I_{\mathrm{BC\_limit}}$ is the maximum current limit for battery charging, $I_{\mathrm{BD_limit}}$ is the maximum current limit for battery discharging, I^*_B is the reference current for a battery converter, I_B is the detected battery current, and D^* is the duty ratio for a dc/dc converter. As shown in Fig. 8, the charging/discharging of a battery converter is determined by I^*_B, which is the sum of the charging controller output and discharging controller output

$$I^*_B = I_{r1} + I_{r2}. \tag{2}$$

When $I^*_B > 0$, the battery converter is used for discharging. When $I^*_B < 0$, the battery converter is used for charging. Hence, the seamless switching between two modes is realized and the hysteresis is not necessary.

As shown in Fig. 8, the overcharging protection and overdischarging protection have been taken into account by introducing V_{BH} and V_{BL}.

D. Power Rating Requirements for the Elements

In the design of the system, the following power rating requirements must be fulfilled to ensure that the proposed control methods can be realized effectively and the system operates safely and stably.

1) The maximum discharging power of batteries should be higher than the power demand of critical local loads, which means that the normal operation of critical loads is ensured even in islanding mode:

$$P_{\mathrm{\_battery\_dischfarging\_max}} \geq P_{\mathrm{\_critical\_load}}. \tag{3}$$

2) The power rating of dc/ac converters must be higher than the sum of maximum local load power and maximum battery charging power to ensure the normal operation of the system in the condition without PV power

$$P_{\mathrm{\_dc/ac\_rating}} \geq (P_{\mathrm{\_load\_max}} + P_{\mathrm{\_battery\_charging\_max}}). \tag{4}$$

3) The maximum available power of PV panels should be greater than the sum of maximum local load power and maximum battery charging power to ensure that the grid-connected power generation can be realized

$$P_{\mathrm{\_PV\_max}} \geq (P_{\mathrm{\_load\_max}} + P_{\mathrm{\_battery\_charging\_max}}). \tag{5}$$

4) The dc/ac converters should be designed to be capable of transferring maximum PV power to the ac grid

$$P_{\mathrm{\_dc/ac\_rating}} \geq P_{\mathrm{\_PV\_max}}. \tag{6}$$

5) The power rating of dc/ac converters should be greater than maximum battery discharging, which ensures that the system can switch from Mode I to Mode II automatically

$$P_{\mathrm{\_dc/ac\_rating}} \geq P_{\mathrm{\_battery\_discharging\_max}}. \tag{7}$$

IV. Experimental Validation

In order to validate the proposed control methods, experimental tests have been carried out on an experimental setup in a laboratory. The configuration and power flow direction setup are shown in Fig. 9.

As shown in Fig. 9, the experimental setup consists of three PV generation units, two grid-connection units, one energy storage unit, and one local resistor load, which are connected through a dc bus. The dc bus voltage is set at 180, 190, 200, and 210 V according to different operation modes. The rms value of the ac grid voltage is 110 V. The selection of experiment voltages (dc 180–210 V, ac 110 V) is mainly based on the safety considerations for laboratory experiments. In a real system, the

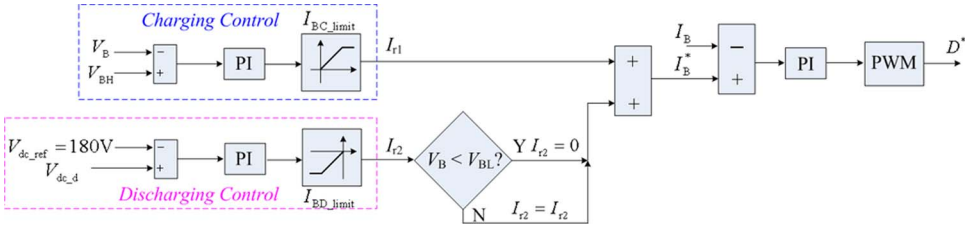

Fig. 8. Control diagram of a dc/dc converter for a battery.

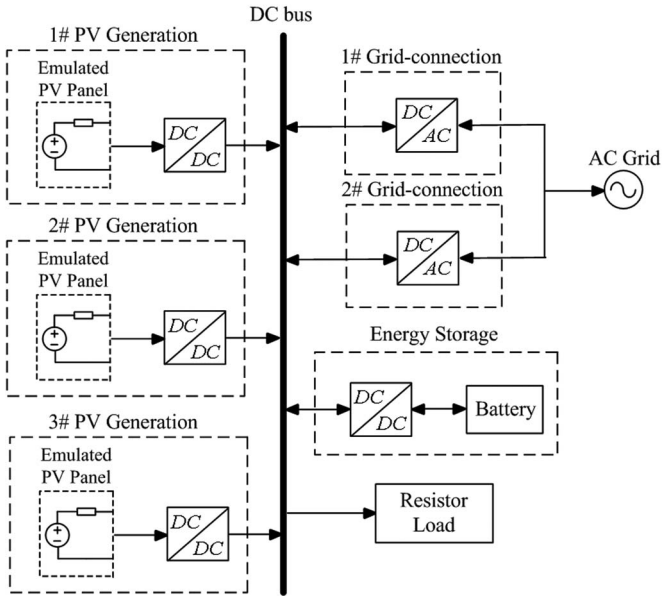

Fig. 9. Configuration of the experimental setup.

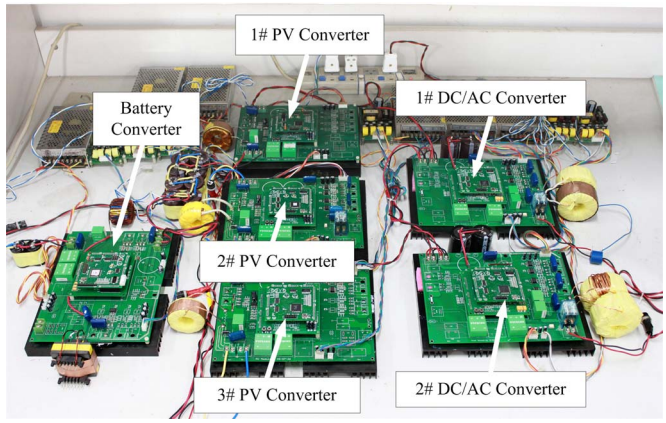

Fig. 10. Photo of the experimental setup.

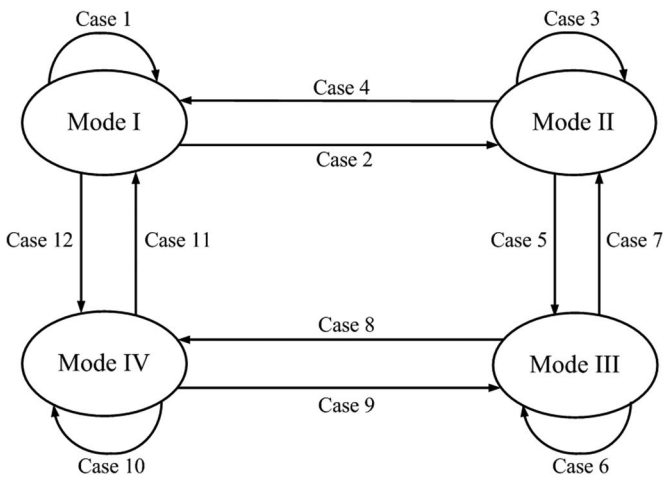

Fig. 11. Cases of the experimental tests.

experiment voltages can be enhanced to dc 360–420 V and ac 220 V, since the power converters have enough power ratings.

Each PV generation unit is constituted of an emulated PV panel and a boost dc/dc converter. A dc voltage source (200 V) series-connected with a resistor (33.3 Ω) is used to emulate a string of PV panels. Hence, when the PV generation unit is operating with MPPT control, the maximum power is 300 W and the corresponding MPPT voltage is 100 V. MPPT control and CV control for PV generation are realized by the boost dc/dc converter. Two 500-W bidirectional dc/ac converters are used as the grid-connection unit, which employs a nonisolated single-phase H-bridge topology. A bidirectional Buck-Boost converter and a battery compose the energy storage unit. The nominal voltage of a battery is 48 V_{dc}. The maximum charging current and maximum discharging current are 1.2 and 10 A, respectively, which are determined by the battery capacity (12 Ah). The photo of the experimental setup is shown in Fig. 10.

Experimental tests have been carried out in terms of steady-state performance, dynamic performance within one mode (at load power changes or PV power changes), and transient performance between different modes. There are total 12 cases, which are illustrated in Fig. 11.

In order to simplify the experimental circuits, only 1# PV generation unit (including emulated PV panel and PV converter) and 2# PV generation unit are connected with a dc bus in the experimental tests of Cases 1–9, while 3# PV generation unit is disconnected. In the experimental tests of Cases 10–12, all the three PV generation units are connected with a dc bus and the dc/ac converters do not work.

A. Test Results in Mode I (Case 1)

Experimental results during load changes in Mode I are shown in Fig. 12. In Fig. 12, $V_{\rm bus}$ is the dc bus voltage, $I_{B\_\rm Discharge}$ is the discharging current of a battery, $V_{\rm PV1}$ is the input voltage of 1# PV converter, and $V_{\rm PV2}$ is the input voltage of 2# PV converter. As shown in Fig. 12, the input voltages of 1# and 2# PV converters are kept at 100 V, which means that both of 1#

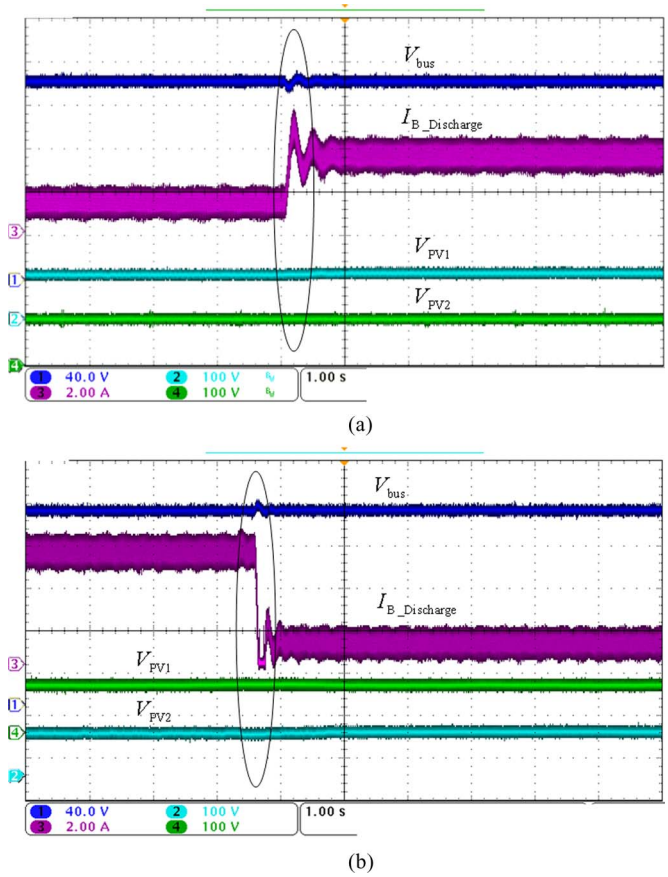

Fig. 12. Experimental results during load changes in Mode I. (a) Dynamic response at load power increase. (b) Dynamic response at load power decrease.

and 2# PV generation units operate at MPPT mode. Since the PV power is greater than the local load power in Mode I, the dc bus voltage is regulated at 180 V by battery discharging. It can be seen that the dc bus voltage is controlled very well even during load change transitions.

B. Test Results in the Transition From Mode I to Mode II (Case 2)

Experimental results in the transition from Mode I to Mode II are shown in Fig. 13. To simplify the experimental circuits, only one grid-connected dc/ac converter is used in this case. In Fig. 13, $V_{\rm bus}$ is the dc bus voltage, $I_{B\_\rm Discharge}$ is the discharging current of a battery, $i_{\rm grid}$ is the ac grid current of the dc/ac converter, and $v_{\rm grid}$ is the ac grid voltage. As shown in Fig. 13, after the grid-connected dc/ac converter starts, the dc bus voltage increases and the battery discharging stops. Then, the dc bus voltage is controlled at 190 V by the rectification of the dc/ac converter.

C. Test Results in Mode II (Case 3)

Dynamic experimental results during load changes with two grid-connected dc/ac converters in Mode II are shown in Fig. 14. $i_{\rm grid1}$ and $i_{\rm grid2}$ are the ac grid currents of 1# and 2# dc/ac converters, respectively. When the load power increases, 2# dc/ac converter changes from nonfull load operation to full load operation and 1# dc/ac converter changes from standby mode to nonfull load operation due to $K_{d1} > K_{d2}$ (the dc bus voltage sampling coefficients). When the load power decreases, 1# dc/ac converter changes from nonfull load operation to standby mode and 2# dc/ac converter changes from full load operation to nonfull load operation due to $K_{d1} > K_{d2}$. The parallel control method for modular dc/ac converters is described in [25]. As can be seen, the dynamic responses of the dc/ac converters to local

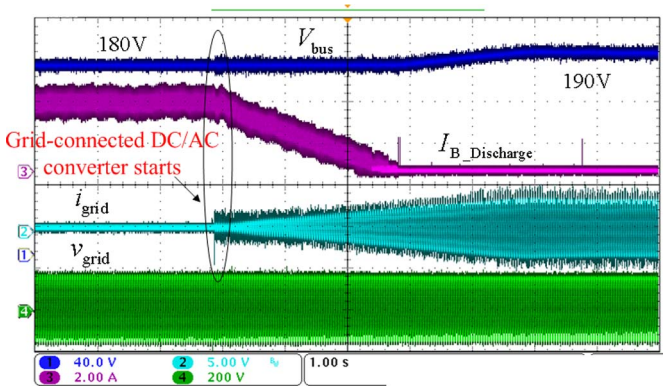

Fig. 13. Experimental results in the transition from Mode I to Mode II.

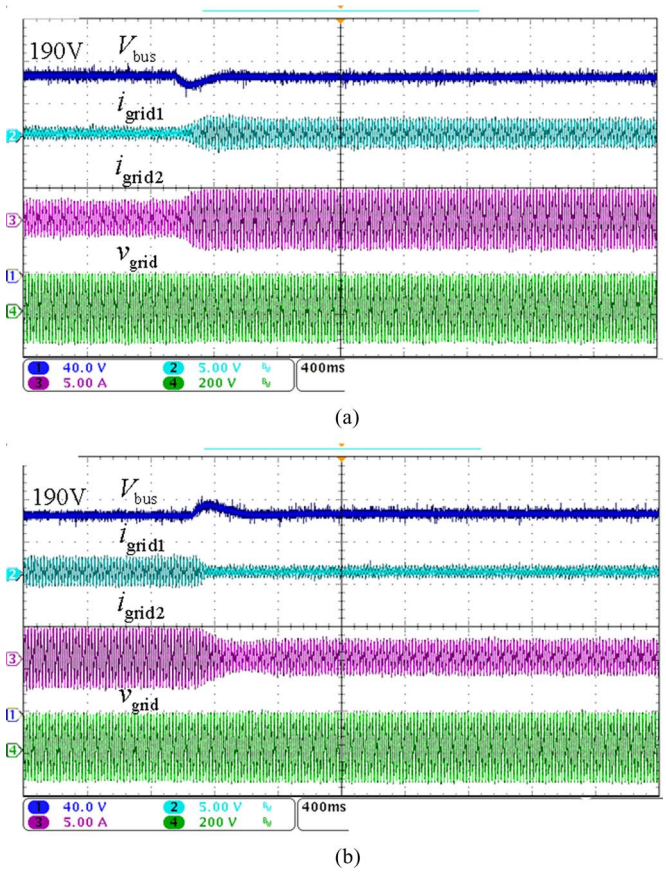

Fig. 14. Experimental results during load changes with two modular dc/ac converters in Mode II. (a) Dynamic response at load power increase. (b) Dynamic response at load power decrease.

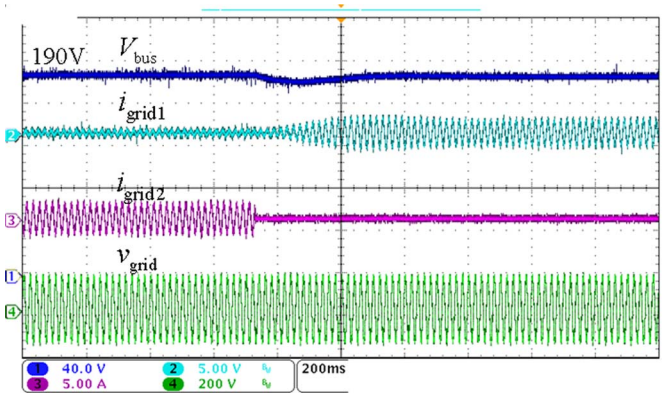

Fig. 15. Experimental results during a fault occurring.

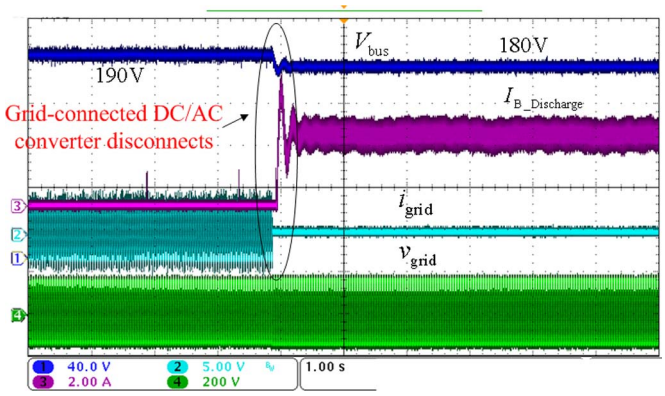

Fig. 16. Experimental results in the transition from Mode II to Mode I.

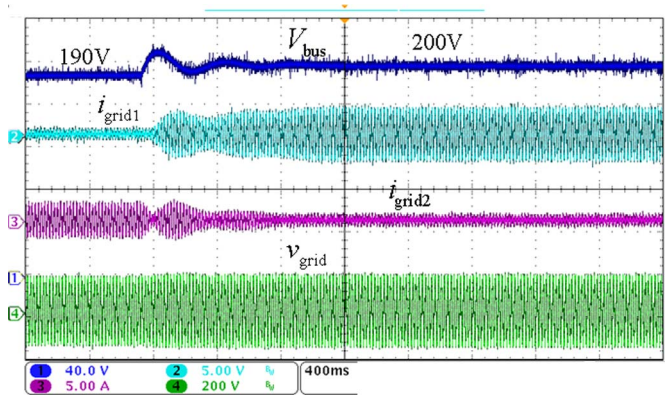

Fig. 17. Experimental results in the transition from Mode II to Mode III with two dc/ac converters.

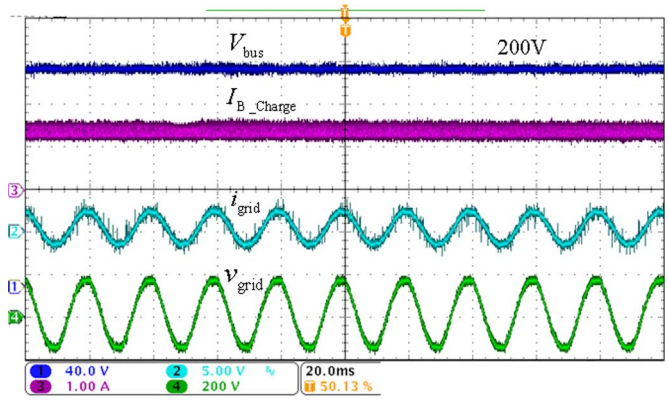

Fig. 18. Steady-state experimental results in Mode III.

load power changes are very fast and only a small fluctuation occurs on the dc bus voltage.

Fig. 15 shows the experimental results during a fault occurring. As can be seen, when 2# dc/ac converter is shut down due to fault, 1# dc/ac converter moves from standby mode to normal operation quickly and stably, which realizes hot swapping and enhances the system redundancy.

D. Test Results in the Transition From Mode II to Mode I (Case 4)

Experimental results in the transition from Mode II to Mode I are shown in Fig. 16. In the initial state, 1# and 2# PV generation units operate at MPPT mode, a dc/ac converter works as a rectifier to regulate the dc bus voltage, and the energy storage unit does not work. As shown in Fig. 16, after the system is disconnected with ac grid, the dc bus voltage decreases because the local load power is greater than the PV power. Then, the battery dc/dc converter is triggered and starts battery discharging. Finally, the dc bus voltage is regulated at 180 V by battery discharging.

E. Test Results in the Transition From Mode II to Mode III (Case 5)

Experimental results in the transition from Mode II to Mode III with two dc/ac converters are shown in Fig. 17. Due to $K_{d1} > K_{d2}$, as rectified power increases 2# dc/ac converter reaches full load operation first during the rectification in Mode II and 1# dc/ac converter reaches full load operation first as inverted power increases during the inversion in Mode III.

F. Test Results in Mode III (Case 6)

Steady-state experimental results in Mode III are shown in Fig. 18. In this case, since the PV power is greater than local load power, the dc/ac converter works as an inverter (ac grid voltage and ac grid current are in phase) and controls the dc bus voltage at 200 V. In addition, the battery is charged with constant current (1.2 A).

Experimental results on battery overcharging protection in Mode III are shown in Fig. 19. When the battery voltage is detected to be equal to V_{BH}, which means that the SoC of a battery reaches 95%, the constant current charging is stopped to avoid overcharging. Correspondingly, ac grid current increases.

Experimental results during load changes in Mode III with two dc/ac converters are shown in Fig. 20. As can be seen, regardless whether the local load power increases or decreases the dc bus voltage has been kept at the reference voltage with small fluctuations.

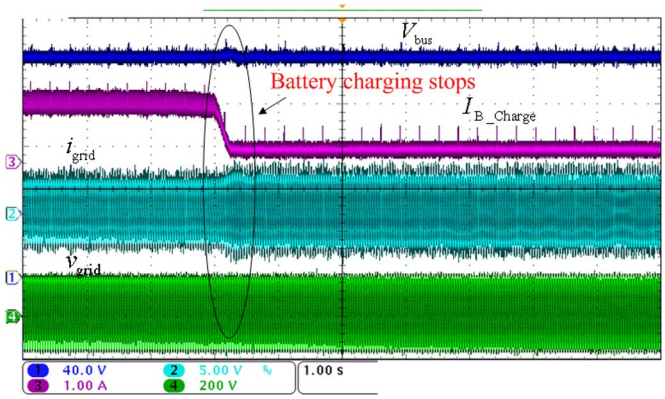

Fig. 19. Experimental results on battery overcharging protection in Mode III.

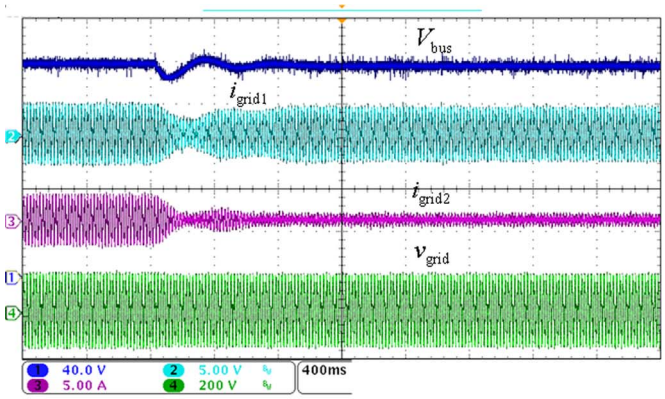

(a)

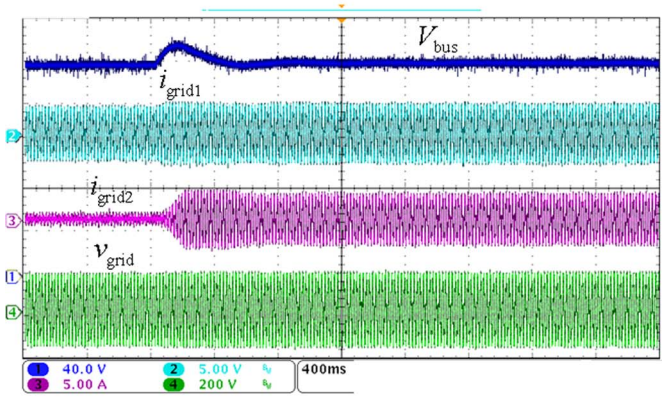

(b)

Fig. 20. Experimental results during load changes in Mode III with two dc/ac converters. (a) Dynamic response at load power increase. (b) Dynamic response at load power decrease.

G. Test Results in the Transition From Mode III to Mode II (Case 7)

Experimental results in the transition from Mode III to Mode II with two dc/ac converters are shown in Fig. 21. Due to $K_{d1} > K_{d2}$, as rectified power increases 2# dc/ac converter reaches full load operation first during the rectification in Mode II and 1# dc/ac converter reaches full load operation first as inverted power increases during the inversion in Mode III.

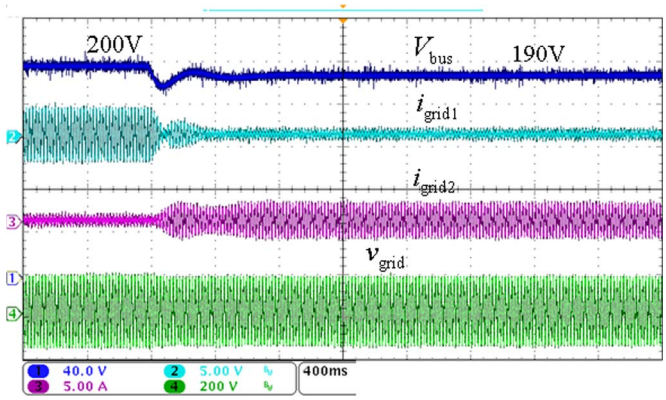

Fig. 21. Experimental results in the transition from Mode III to Mode II with two dc/ac converters.

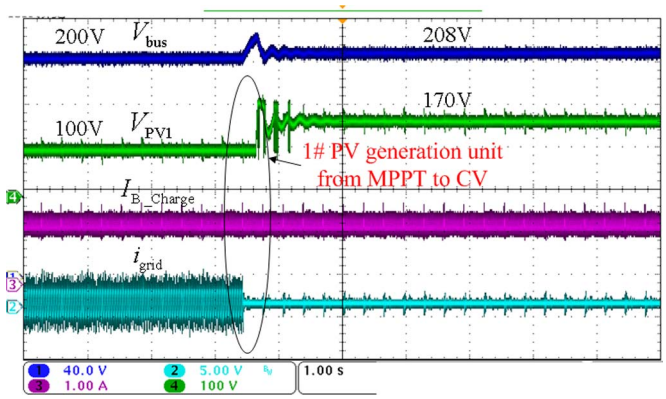

Fig. 22. Experimental results in the transition from Mode III to Mode IV.

H. Test Results in the Transition From Mode III to Mode IV (Case 8)

Experimental results in the transition from Mode III to Mode IV are shown in Fig. 22. In the initial state, 1# and 2# PV generation units work at MPPT mode (PV converter input voltage 100 V), the dc bus voltage is regulated at 200 V by the inversion of a grid-connected dc/ac converter, and the battery is under constant current charging. As shown in Fig. 22, when the system is disconnected with ac grid, the dc bus voltage increases because the PV power is greater than the local load power. In order to maintain power balance, 1# PV generation unit changes from MPPT mode to CV mode (PV converter input voltage 170 V) and controls the dc bus voltage at 208 V. Although the reference dc bus voltage is 210 V, 2 V error exists due to the sampling coefficient variations. Since the battery has not been fully charged, the constant current charging continues. As shown in Fig. 22, some small oscillations on V_{PV1} occur during the mode switching transition, which does not cause instability.

I. Test Results in the Transition from Mode IV to Mode III (Case 9)

Experimental results in the transition from Mode IV to Mode III are shown in Fig. 23. In the initial state, 2# PV generation unit works at MPPT mode, 1# PV generation unit works

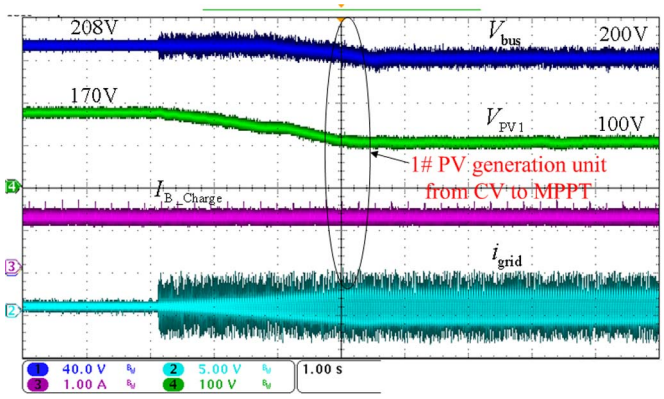

Fig. 23. Experimental results in the transition from Mode IV to Mode III.

at CV mode (PV converter input voltage 170 V) and regulates the dc bus voltage at 208 V, the dc/ac converter does not work, and the battery is under constant current charging. As shown in Fig. 23, when the system is connected with ac grid, the dc bus voltage is regulated at 200 V by the inversion of the dc/ac converter and 1# PV generation unit changes from CV mode to MPPT mode (PV converter input voltage 100 V). Since the battery has not been fully charged, the constant current charging continues.

J. Test Results in Mode IV (Case 10)

In Mode IV, the system is disconnected with ac grid and operates as an island. Since the maximum PV power is greater than the local load power, only one PV generation unit works at CV mode to maintain power balance, and the other PV generation units work at MPPT mode or at standby mode.

Independent CV operations of 1#, 2#, and 3# PV generation units have been tested. Although the reference dc bus voltage is 210 V, the real dc bus voltage is regulated at 208 V, 209 V, and 214 V, respectively, due to different sampling coefficients. Hence, when the load power decrease, the three PV generation units change from MPPT mode to CV mode or standby mode gradually according to the following sequence 1# $\rightarrow$2# $\rightarrow$ 3#.

Experimental results at load power changes in Mode IV are shown in Fig. 24. In Fig. 24, $V_{\rm bus}$ is the dc bus voltage, $V_{\rm PV1}$ is the input voltage of 1# PV converter, $V_{\rm PV2}$ is the input voltage of 2# PV converter, and $V_{\rm PV3}$ is the input voltage of 3# PV converter.

Experimental results at load power decrease in Mode IV are shown in Fig. 24(a). In the initial state, 1# PV generation unit works at CV mode (PV converter input voltage 140 V) and regulates the dc bus voltage at 208 V, and 2# and 3# PV generation units work at MPPT mode (PV converter input voltage 100 V). When the load decrease occurs, since the dc bus voltage sampling coefficient of 2# PV generation unit is greater than the one of 3# PV generation unit, 2# PV generation unit changes from MPPT mode to CV mode (PV converter input voltage 150 V) and regulates the dc bus voltage at 209 V, 1# PV generation unit changes from CV mode to standby mode (PV converter input voltage 200 V) and does not generate power, and 3# PV generation unit keeps at MPPT mode.

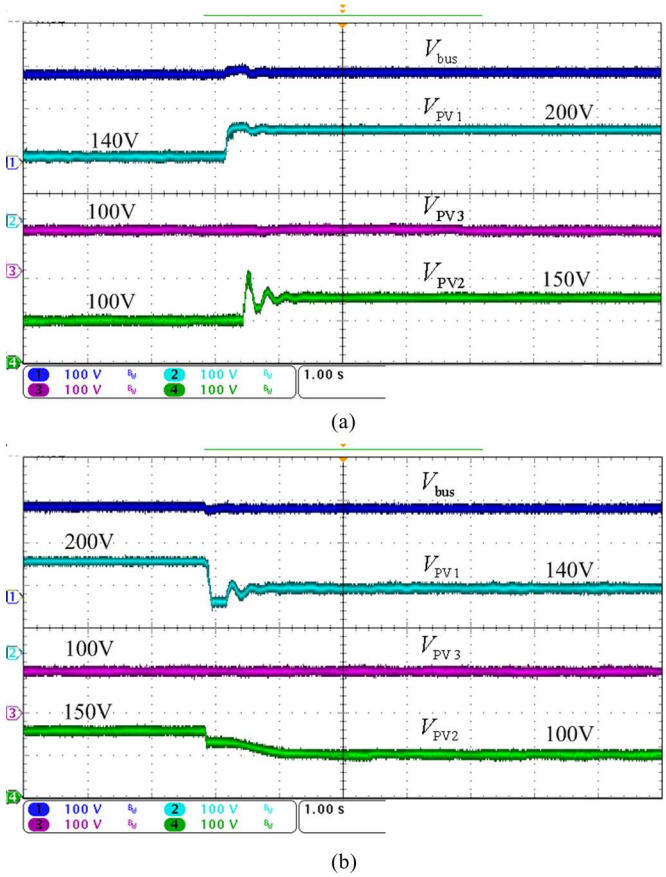

Fig. 24. Experimental results at load power changes in Mode IV. (a) Dynamic response at load power decrease. (b) Dynamic response at load power increase.

Experimental results at load power increase in Mode IV are shown in Fig. 24(b). In the initial state, 1# PV generation unit works at standby mode (PV converter input voltage 200 V); 2# PV generation unit works at CV mode (PV converter input voltage 150 V) and regulates the dc bus voltage at 209 V; and 3# PV generation unit works at MPPT mode (PV converter input voltage 100 V). When the load increase occurs, 1# PV generation unit changes from standby mode to CV mode (PV converter input voltage 140 V) and regulates the dc bus voltage at 208 V; 2# PV generation unit changes from CV mode to MPPT mode; and 3# PV generation unit keeps at MPPT mode.

Experimental results at PV power changes in Mode IV are shown in Fig. 25. In Fig. 25, $I_{\rm PV3}$ is the input current of 3# PV converter. PV power changes are realized by changing the series-connected resistor as shown in Fig. 9.

Experimental results at PV power increase in Mode IV are shown in Fig. 25(a). In the initial state, 1# PV generation unit works at standby mode, 2# PV generation unit works at CV mode (PV converter input voltage 120 V), and 3# PV generation unit works at MPPT mode (PV converter input voltage 100 V and input current 3 A). When a 150-W power increase of 3# PV generation unit occurs, 3# PV generation unit keeps at MPPT mode (PV converter input voltage 100 V) and the input current of 3# PV converter increases to 4.5 A. The input voltage of 2# PV converter increases to 180 V, which means that the generated

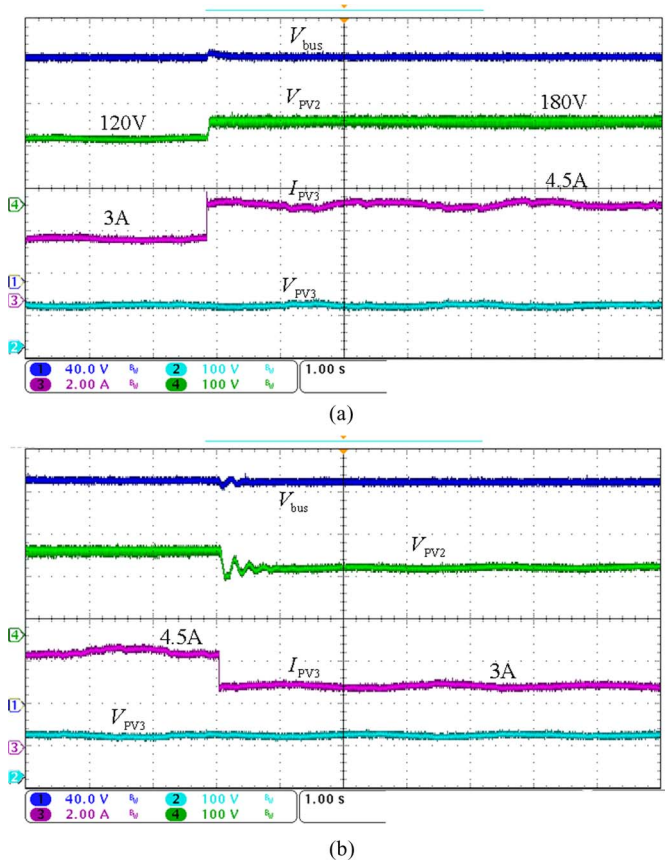

Fig. 25. Experimental results during PV power changes in Mode IV. (a) Dynamic response at PV power increase. (b) Dynamic response at PV power decrease.

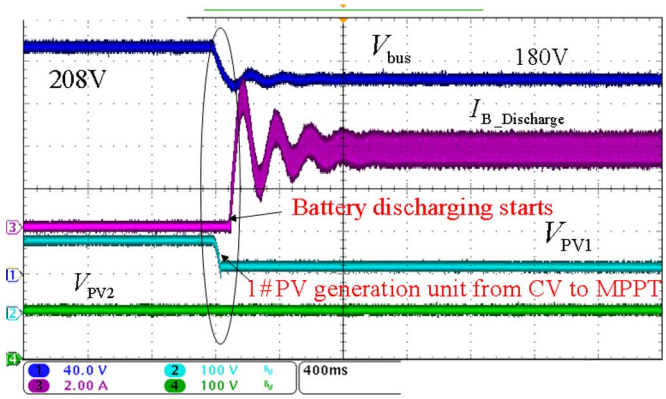

Fig. 26. Experimental results in the transition from Mode IV to Mode I.

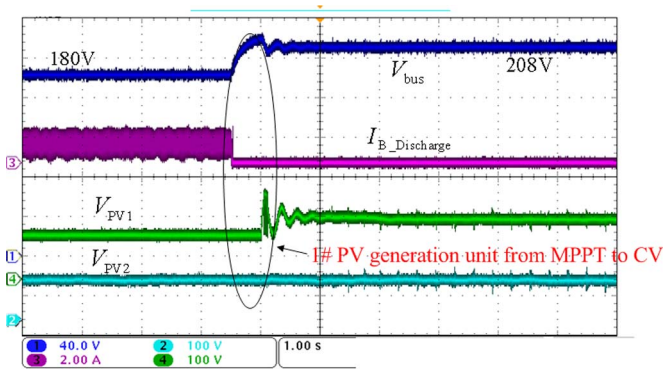

Fig. 27. Experimental results in the transition from Mode I to Mode IV.

power of 2# PV generation unit is reduced. However, 2# PV generation unit still keeps at CV mode and regulates the dc bus voltage at 209 V.

Experimental results at PV power decrease in Mode IV are shown in Fig. 25(b). In the initial state, 1# PV generation unit works at standby mode, 2# PV generation unit works at CV mode, and 3# PV generation unit works at MPPT mode (PV converter input voltage 100 V and input current 4.5 A). When a 150-W power decrease of 3# PV generation unit occurs, 3# PV generation unit keeps at MPPT mode (PV converter input voltage 100 V) and the input current of 3# PV converter decreases to 3 A. The input voltage of 2# PV converter decreases, which means that the generated power of 2# PV generation unit is enhanced. However, 2# PV generation unit still keeps at CV mode and regulates the dc bus voltage at 209 V.

As shown in Figs. 24 and 25, the dynamic responses to load power changes and PV power changes are very fast and the overshoots are not severe under the proposed control methods.

K. Test Results in the Transition From Mode IV to Mode I (Case 11)

Experimental results in the transition from Mode IV to Mode I are shown in Fig. 26. In the initial state, the system is disconnected with ac grid; the energy storage unit does not work; 1# PV generation unit works at CV mode (PV converter input voltage 130 V) and regulates the dc bus voltage at 208 V; and 2# and 3# PV generation units work with MPPT. When load power increase occurs, 1# PV generation unit changes from CV mode to MPPT mode. However, the PV power is still lower than the load power demands and the dc bus voltage decreases continuously. About 1 s later, the battery discharging is started and the dc bus voltage is regulated at 180 V.

L. Test Results in the Transition From Mode I to Mode IV (Case 12)

Experimental results in the transition from Mode I to Mode IV are shown in Fig. 27. In the initial state, the system is disconnected with ac grid; 1#, 2#, and 3# PV generation units work at MPPT mode; and the energy storage unit controls the dc bus voltage at 180 V by battery discharging. When load power decrease occurs, the dc bus voltage increases and the battery discharging is stopped; 1# PV generation unit changes from MPPT mode to CV mode (PV converter input voltage 140 V) and regulates the dc bus voltage at 208 V; and 2# and 3# PV generation units keep at MPPT mode.

V. Conclusion

In this paper, a distributed control strategy based on DBS for a modular PV generation system with battery energy storage is proposed. The dc bus voltage level is employed as an information carrier to represent different operation modes and

determine mode switching. Control methods for modular PV converters, modular grid-connected dc/ac converters, and a battery converter are developed, respectively.

Experimental tests in terms of steady-state performances and dynamic performances (transitions between different modes, load power changes, and PV power changes) have been carried out on an experimental setup. The results demonstrate that: 1) the developed system operates stably in islanding mode and grid-connected mode with the proposed control strategy; 2) smooth transitions between different modes are realized without severe oscillations of voltage or current; 3) the power balance of the system under extreme condition (the islanding mode with a full-charged battery) is guaranteed by the proposed control method for modular PV converters; and 4) the overcharging and overdischarging faults of batteries are avoided by the developed control method for a battery converter. In other words, the practical feasibility and the effectiveness of the proposed control strategies have been validated by the experiments.

This modular PV generation system with a distributed control strategy can be applied in residential PV generation in rural area and building integrated PV generation, and also the distributed control strategy can be applied for dc nanogrid and dc microgrids.

REFERENCES

[1] R. H. Lasseter, A. Akhil, C. Marnay, J. Stevens, J. Dagle, R. Guttromson, A. S. Meliopoulous, R. Yinger, and J. Eto, "White paper on integration of distributed energy resources, the CERTS microgrid concept," in *Consortium for Electric Reliability Technology Solutions*, Gray, Davis, Governor, Apr. 2002, pp. 1–27.

[2] R. H. Lasseter and P. Paigi, "Microgrid: A conceptual solution," in *Proc. IEEE Power Electron. Spec. Conf. (PESC'04)*, Jun., vol. 6, pp. 4285–4290.

[3] Y. W. Li and C. N. Kao, "An accurate power control strategy for power-electronics-interfaced distributed generation units operating in a low-voltage multibus microgrid," *IEEE Trans. Power Electron.*, vol. 24, no. 12, pp. 2977–2988, Dec. 2009.

[4] H. Kakigano, Y. Miura, and T. Ise, "Configuration and control of a DC microgrid for residential houses," in *Proc. IEEE Transmis. Distrib. Conf. Expo.: Asia Pacific*, Oct. 2009, pp. 1–4.

[5] H. Kakigano, Y. Miura, T. Ise, and R. Uchida, "DC micro-grid for super high quality distribution-system configuration and control of distributed generations and energy storage devices," in *Proc. IEEE Power Electron. Spec. Conf. (PESC'06)*, pp. 1–7.

[6] S. B. Kjaer, J. K. Pedersen, and F. Blaabjerg, "A review of single-phase grid-connected inverters for photovoltaic modules," *IEEE Trans. Ind. Appl.*, vol. 41, no. 5, pp. 1292–1306, Sep./Oct. 2005.

[7] Q. Li and P. Wolfs, "A review of the single phase photovoltaic module integrated converter topologies with three different DC link configurations," *IEEE Trans. Power Electron.*, vol. 23, no. 3, pp. 1320–1333, May 2008.

[8] E. Ozdemir and F. Kavaslar, "A new multifunctional power converter for grid connected residential photovoltaic applications," in *Proc. IEEE Energy Conversion Congress and Exposition (ECCE'09)*, Sep. 2009, pp. 2650–2656.

[9] L. Ma, K. Sun, R. Teodorescu, J. M. Guerrero, and X. Jin, "An integrated multifunction DC/DC converter for PV generation systems," in *Proc. IEEE Int. Symp. Industrial Electronics (ISIE'10)*, pp. 2205–2210.

[10] Y. Gurkaynak and A. Khaligh, "Control and power management of a grid connected residential photovoltaic system with plug-in hybrid electric vehicle (PHEV) load," in *Proc. IEEE Appl. Power Electron. Conf. (APEC'09)*, pp. 2086–2091.

[11] G. M. Tina and F. Pappalardo, "Grid-connected photovoltaic system with battery storage system into market perspective," in *Proc. IEEE Power and Energy Society/Industry Application Society Conf. Sustainable Alternative Energy (SAE)*, Sep. 2009, pp. 1–7.

[12] T. Shimada, Y. Ueda, and K. Kurokawa, "Look-ahead equalizing charge planning for grid-connected photovoltaic systems with battery storages," in *Proc. IEEE Photovoltaic Spec. Conf. (PVSC'08)*, 2008, pp. 1–3.

[13] F. Giraud and Z. M. Salameh, "Steady-state performance of a grid-connected rooftop hybrid wind–photovoltaic power system with battery storage," *IEEE Trans. Energy Convers.*, vol. 16, no. 1, pp. 1–7, Mar. 2001.

[14] R. Carbone, "Grid-connected photovoltaic systems with energy storage," in *Proc. Int. Conf. Clean Electrical Power (ICCEP'09)*, Jun. 2009, pp. 760–767.

[15] T. Kato, H. Yamawaki, and Y. Suzuoki, "A study on dumping power flow fluctuation at grid-connection point of residential micro-grid with clustered photovoltaic power generation systems," in *Proc. IEEE PES/IAS Conf. Sustainable Alternative Energy (SAE)*, Sep. 2009, pp. 1–6.

[16] H. Valderrama-Blavi, J. M. Bosque-Moncusí, L. Marroyo, F Guinjoan, J. A. Barrado, and L. Martínez-Salamero, "Adapting a low voltage PEM fuel-cell to domestic grid-connected PV system," in *Proc. IEEE Ind. Electron. Ann. Conf. Soc.*, 2009, pp. 160–165.

[17] Z. Jiang and R. A. Dougal, "Hierarchical microgrid paradigm for integration of distributed energy resources," in *Proc. IEEE Power Energy Soc. Gen. Meet.—Convers. Del. Electr. Energy in the 21st Century*, Jul. 2008, pp. 1–8.

[18] M. E. Glavin, P. K. W. Chan, and W. G. Hurley, "Optimization of autonomous hybrid energy storage system for photovoltaic applications," in *Proc. IEEE Energy Conversion Congress and Exposition (ECCE'09)*, pp. 1417–1424.

[19] H. Nakayama, E. Hiraki, T. Tanaka, N. Koda, N. Takahashi, and S. Noda, "Stand-alone photovoltaic generation system with combined storage system using EDLC," in *Proc. IEEE Ind. Electron. Ann. Conf. Soc.*, 2009, pp. 883–888.

[20] J. Eduardo, M. S. Paiva Adriano, and S. Carvalho, "An integrated hybrid power system based on renewable energy sources," in *Proc. IEEE IECON2009*, Nov. 2009, pp. 4548–4554.

[21] S. J. Chiang, H.-J. Shieh, and M.-C. Chen, "Modeling and control of PV charger system with SEPIC converter," *IEEE Trans. Ind. Electron.*, vol. 56, no. 11, pp. 4344–4353, Nov. 2009.

[22] D. D.-C. Lu and V. G. Agelidis, "Photovoltaic-battery-powered DC bus system for common portable electronic devices," *IEEE Trans. Power Electron.*, vol. 24, no. 3, pp. 849–855, Mar. 2009.

[23] J. Bryan, R. Duke, and S. Round, "Decentralized generator scheduling in a nanogrid using DC bus signalling," in *Proc. IEEE Power Eng. Soc. Summer Meet.*, Jun. 2004, vol. 1, pp. 977–982.

[24] J. Schonberger, R. Duke, and S. D. Round, "DC bus signalling: A distributed control strategy for a hybrid renewable nanogrid," *IEEE Trans. Ind. Electron.*, vol. 53, no. 5, pp. 1453–1460, Oct. 2006.

[25] L. Zhang, K. Sun, Y. Xing, L. Feng, and H. Ge, "A modular grid-connected photovoltaic generation system based on DC bus," *IEEE Trans. Power Electron.*, vol. 26, no. 2, pp. 523–531, Feb. 2011.

Kai Sun received the B.E., M.E., and Ph.D. degrees in electrical engineering all from Tsinghua University, Beijing, China, in 2000, 2002, and 2006, respectively.

In 2006, he joined the Faculty of Tsinghua University as a Lecturer of Electrical Engineering. From September 2009 to August 2010, he was a Visiting Scholar of Electrical Engineering at Institute of Energy Technology, Aalborg University, Denmark. He is currently with Tsinghua University, Beijing, China. His research interests include power converters, ac motor drives, and renewable generation systems.

Li Zhang was born in Jiangsu, China, in 1985. He received the B.S. degree in electrical engineering from the Nanjing University of Aeronautics and Astronautics (NUAA), Nanjing, China, in 2007, where he is currently working toward the Ph.D. degree in electrical engineering in Jiangsu Key Laboratory of New Energy Generation and Power Conversion.

His research interests include control of dc–ac converter, modular converter systems, and distributed generation technologies.

Yan Xing (M'03) was born in Shandong, China, in 1964. She received the B.S. and M.S. degrees in automation and electrical engineering from Tsinghua University, Beijing, China, in 1985 and 1988, respectively, and the Ph.D. degree in electrical engineering from the Nanjing University of Aeronautics and Astronautics (NUAA), Nanjing, China, in 2000.

Since 1988, she has been with the Faculty of Electrical Engineering, NUAA, and is currently a Professor with Jiangsu Key Laboratory of New Energy Generation and Power Conversion, NUAA. She has authored more than 60 technical papers published in journals and conference proceedings and has also published three books. Her research interests include topology and control for dc-dc and dc-ac converters.

Dr. Xing is an Associate Editor for the IEEE TRANSACTIONS ON POWER ELECTRONICS. She is a member of Renewable Energy Systems Technical Committee of IEEE IES.

Josep M. Guerrero (S'01–M'04–SM'08) received the B.S. degree in telecommunications engineering, the M.S. degree in electronics engineering, and the Ph.D. degree in power electronics from the Technical University of Catalonia, Barcelona, Spain, in 1997, 2000, and 2003, respectively.

He is an Associate Professor with the Department of Automatic Control Systems and Computer Engineering, Technical University of Catalonia, Barcelona, where he currently teaches courses on digital signal processing, FPGAs, microprocessors, and renewable energy. Since 2004, he has been responsible for the Renewable Energy Laboratory, Escola Industrial de Barcelona. He has been a visiting Professor at Zhejiang University, China, and University of Cergy-Pontoise, France. Since 2011 he is a Professor at the Department of Energy Technology, Aalborg Universiy, Denmark. His research interests include power electronics converters for distributed generation and distributed energy storage systems, control and management of microgrids and islanded minigrids, and photovoltaic and wind power plants control.

Dr. Guerrero is an Associate Editor for the IEEE TRANSACTIONS ON POWER ELECTRONICS and IEEE TRANSACTIONS ON INDUSTRIAL ELECTRONICS. He has been Guest Editor of the IEEE Transactions on Power Electronics Special Issues: Power Electrics for Wind Energy Conversion and Power Electronics for Microgrids; and the IEEE Transactions on Industrial Electronics Special Sections: Uninterruptible Power Supplies (UPS) systems, Renewable Energy Systems, Distributed Generation and Microgrids, and Industrial Applications and Implementation Issues of the Kalman Filter. He currently chairs the Renewable Energy Systems Technical Committee of IEEE IES. He is an elected IEEE IES Adcom member.